01 Jun 2019

Slightly Fluorination of Al_2O_3 ALD Coating on $Li_{1.2}Mn_{0.54}Co_{0.13}Ni_{0.13}O_2$ Electrodes: Interface Reaction to Create Stable Solid Permeable Interphase Layer

Han Yu

Yan Gao

Xinhua Liang
Missouri University of Science and Technology, liangxin@mst.edu

Recommended Citation

H. Yu et al., "Slightly Fluorination of Al_2O_3 ALD Coating on $Li_{1.2}Mn_{0.54}Co_{0.13}Ni_{0.13}O_2$ Electrodes: Interface Reaction to Create Stable Solid Permeable Interphase Layer," *Journal of the Electrochemical Society*, vol. 166, no. 10, ECS, Jun 2019.

Slightly Fluorination of Al_2O_3 ALD Coating on $Li_{1.2}Mn_{0.54}Co_{0.13}Ni_{0.13}O_2$ Electrodes: Interface Reaction to Create Stable Solid Permeable Interphase Layer

Han Yu,* Yan Gao,* and Xinhua Liang,z**

Department of Chemical and Biochemical Engineering, Missouri University of Science and Technology, Rolla, Missouri 65409, USA

Improving the performance of cathodes by using surface coatings has proven to be an effective method for improving the stability of Li-ion batteries (LIBs), while a high-quality film satisfying all requirements of electrochemical inertia, chemical stability, and lithium ion conductivity has not been found. In this study, a composite film composed of Al_2O_3 and AlF_3 layers was coated on the surface of $Li_{1.2}Mn_{0.54}Co_{0.13}Ni_{0.13}O_2$ (Li-rich NMC) based electrodes by atomic layer deposition (ALD). By varying the ratio of Al_2O_3 and AlF_3, an optimal coating was achieved. The electrochemical characterization results indicated that the coating with 1 cycle of AlF_3 ALD on 5 cycles of Al_2O_3 ALD ($1AlF_3$-$5Al_2O_3$) significantly improved the cycling stability and alleviated the voltage attenuation problem of Li-rich NMC based electrodes by suppressing side reactions between the electrolyte and electrode, as well as inhibiting the transformation of layered Li_2MnO_3 into a spinel-like phase. After 200 cycles of charge-discharge, the discharge capacity retention of LIB half cells based on $1AlF_3$-$5Al_2O_3$ coated Li-rich NMC electrodes kept at 84%, much higher than that of the uncoated Li-rich NMC (the capacity retention less than 20%).

 [DOI: 10.1149/2.0951910jes]

Manuscript submitted March 6, 2019; revised manuscript received May 21, 2019. Published June 13, 2019.

As one of the main power sources of portable electronic devices, rechargeable Li-ion batteries (LIBs) are very important in our daily life. With a wider range of applications, such as electric vehicles, LIBs with longer cycle life and higher power density are urgently needed.[1–4] Li-rich oxides with layered structure, $xLi_2MnO_3 \cdot (1\text{-}x)LiMO_2$ (M = Mn, Co, Ni), also known as Li-rich NMC, can deliver a discharge capacity over 250 mAh/g within a voltage window of 2.0 V−4.8 V (vs. Li/Li^+). Li-rich NMC has attracted great attention as the next-generation of cathode material for high energy LIBs.[5–8] However, Li-rich NMC suffers from a series of aging problems, which hinder the commercial applications. Firstly, the release of O_2 at high voltage during the first charging process results in thermal instability of the host materials.[9] Secondly, charging to high voltage (e.g., 4.6 V−4.8 V) aggravates the decomposition of electrolyte, leading to undesirable side reactions between the active electrode and electrolyte species, resulting in the formation of solid permeable interphase (SPI) layer.[10,11] Thirdly, during charge-discharge process, transition metal ions move into the Li vacant sites, causing cation disorder and structural change from layered structure to spinel structure and resulting in severe voltage fade.[12] Fourthly, the dissolution of transition metals, such as Mn, leads to severe capacity decay.

To address these issues, many strategies have been employed to improve the electrochemical performance of Li-rich NMC based batteries, including morphology control, element doping, and surface modification. Among the available strategies, the application of a surface coating (e.g., Al_2O_3, AlF_3, and $AlPO_4$) is considered to be an effective method by providing a stable interface between active material and electrolyte.[13–15] Coating mainly plays two roles in improving the electrochemical performance of these cathodes: prevention of direct contact between the electrode and the electrolyte, and suppression of transition metal (especially Mn) dissolution. Al_2O_3 is the most studied coating material and has been shown to suppress side reactions between electrodes and electrolyte as well as mitigate the decomposition of electrolyte.[16–18] It was reported that Al_2O_3 ALD thin film coated on the surface of $LiMn_{1.5}Ni_{0.5}O_4$ (LMNO) electrode dramatically suppressed self-discharge effects as well as the dissolution of transition metals.[16] AlF_3 coating could create some interaction with transition metal elements of Li-rich NMC to form a stable coating, which can promote the stability and lithium diffusion capacity of Li-rich NMC.[19–21] However, normally AlF_3 coating was prepared by wet chemical methods, and the coating was not uniform. No matter it is Al_2O_3 or AlF_3, the thickness of coating must be ultra-thin to get an optimal promotion. If the coating is too thick, there would be a barrier for mass transfer, although it was reported that the fluorination of Al_2O_3 contributed to the increase of discharge capacity.[17] If the coating is too thin, it can't stand for a long time and, normally, after 100 cycles of charge-discharge process, the protection of Al_2O_3 decreased and then the host materials suffered a severe capacity fading, since HF resulted from the decomposition of electrolyte will consume the Al_2O_3 coating. In order to obtain stable performance without sacrificing the rate capacity, the coating should own the properties of chemical stability, electronic conductivity, and Li ion conductivity. As most of the coating layers own one or two of those properties, it is beneficial to combine the merits of two different coatings.

To the best of our knowledge, a strategy of combining two or more coatings' merits has not been reported. In this work, we combined the merits of ultra-thin Al_2O_3 film and AlF_3 film but without sacrificing the electronic conductivity, by coating different thicknesses of AlF_3 ALD films on Al_2O_3 ALD coated NMC electrodes directly. The results showed that the capacity retention of $1AlF_3$-$5Al_2O_3$ NMC (1 cycle of AlF_3 ALD on 5 cycles of Al_2O_3 ALD coated Li-rich NMC electrodes) was much higher than that of uncoated Li-rich NMC. In addition, a much stable discharge voltage suggested that the coated NMC could provide a stable power density.

Experimental

Li-rich NMC electrode fabrication.—The Li-rich NMC electrode was prepared by mixing a slurry of the Li-rich NMC powders (NEI Corp.), super P (Alfa Aesar), and poly (vinylidene fluoride) (PVDF) (Sigma Aldrich) binder in N-methyl-2-pyrrolidone (Sigma Aldrich) solvent with a weight ratio of NMC: super P: PVDF = 8:1:1, and then the slurry was casted on a piece of aluminum foil. The coated foil was heated to 80°C for 10 minutes in air and then dried overnight in a vacuum oven at 120°C. After drying, the coated foil was punched into disks with an area of 0.71 cm^2. A typical loading of the electrodes was about 3.5 mg cm^{-2}.

Atomic layer deposition.—Al_2O_3 and AlF_3 films were directly coated on NMC electrode disks by ALD at 100°C. Trimethylaluminum (TMA) (Sigma Aldrich) and H_2O were used as precursors for Al_2O_3 ALD. A single cycle of Al_2O_3 ALD sequence included: (1) TMA dose for 5 s, (2) wait 30 s for diffusion and reaction, (3) flush chamber

*Electrochemical Society Student Member.
**Electrochemical Society Member.
zE-mail: liangxin@mst.edu

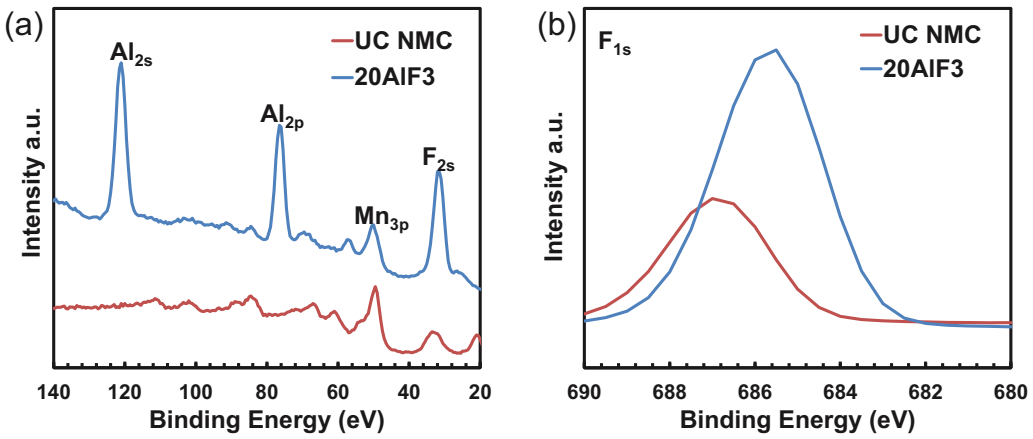

Figure 1. (a) XPS spectra of UC NMC electrode and 20AlF_3 NMC electrode, and (b) high resolution XPS spectra of F_{1s}.

with N_2 for 60 s to remove reaction byproducts (e.g., CH_4) and excess TMA, (4) evacuate chamber for 10 s, (5) H_2O dose for 2 s, (6) wait 30 s for diffusion and reaction, (7) flush chamber with N_2 for 60 s to remove reaction byproducts and excess H_2O, and (8) evacuate chamber for 10 s. AlF_3 films were deposited on NMC electrodes by ALD with TMA and HF-pyridine (Sigma Aldrich) as precursors.[22] The AlF_3 ALD sequence was the same as that of the Al_2O_3 ALD process. All precursors were delivered into the reactor based on their room temperature vapor pressures. In this study, 2, 4, and 6 cycles of Al_2O_3 ALD and 2, 4, 6, and 8 cycles of AlF_3 ALD were coated on NMC electrodes separately. For the composite coating, Al_2O_3 was first coated on NMC electrodes, followed by AlF_3 ALD; total 6 cycles of ALD were carried out, including x cycles of Al_2O_3 ALD followed by (6-x) cycles of AlF_3 ALD. The samples were name as (6-x)AlF_3-xAl_2O_3.

Materials characterizations.—The uncoated and ALD coated NMC electrodes were subjected to X-ray powder diffraction analysis by Philips X-Pert multi-purpose diffractometer (MPD) using Cu Ka radiation with 2q ranging from 5° to 90° at a scanning rate of 2.8 °min^{-1}. A Kratos 165 XPS Scanning Microprobe (Physical Electronics) with a monochromated AlK α source was used for the surface composition analysis.

Electrochemical testing.—CR2032-type coin cells were assembled in an Ar-filled dry glove box. Li metal foil was used as counter electrode in half cells. A 1.0 M solution of $LiPF_6$ dissolved in a mixture of ethylene carbonate (EC) and dimethyl carbonate (DMC) (1:1 in volume) (Sigma Aldrich) was used as electrolyte. A porous polypropylene (PP)/polyethylene (PE)/PP tri-layer film (Celgard Inc.) was used as separator. Galvanostatic charge-discharge cycling was performed on a battery station (Neware Corp.) over a potential range 2.0 V−4.8 V (vs. Li/Li^+) at 25°C at a current density of 0.05C (1C = 250 mAh/g) for the first two cycles and 1C for the subsequent cycles. AC impedance measurements were performed using a signal with amplitude of 5 mV over a frequency range from 500 kHz to 10 mHz. AC impedance spectra were recorded at an open circuit voltage of ∼2.9 V (vs. Li/Li^+).

Results and Discussion

For the easiness of characterization, a NMC electrode was deposited with 20 cycles of AlF_3 ALD. To identify the existence of AlF_3 film, the surface compositions of the uncoated NMC (UC NMC) and 20 cycles AlF_3 coated NMC (20AlF_3 NMC) electrodes were analyzed by XPS, as shown in Fig. 1. Although Al foil was used as the current collector, there was no peak belonging to Al on the UC NMC electrode, so Al foil had no influence on XPS results. For 20AlF_3 NMC, there were two strong peaks at 120 eV and 77 eV belonging to Al_{2s} and Al_{2p}, respectively, and the peak at 31 eV belonged to F_{2s}. Fig. 1b shows a high resolution XPS spectrum of F_{1s}; the peak at 687.1 eV belonged to PVDF and the peak at 685.9eV was related to metal fluoride (AlF_3). These results confirmed the formation of AlF_3 on the surface of NMC electrodes by ALD.

Fig. 2 shows the XRD patterns of the UC NMC and 20AlF_3 NMC electrodes. All the diffraction peaks of both materials can be indexed as NMC with hexagonal α-$NaFeO_2$ structure. The strong peaks of the two patterns at 45° belonged to Al foil. The XRD patterns of UC NMC and 20AlF_3 NMC were very similar, indicating that the AlF_3 coating did not affect the bulk structure of NMC. In addition, no diffraction peaks from AlF_3 were observed in the XRD pattern due to the amorphous state of AlF_3.

Different cycles of Al_2O_3 or AlF_3 were coated on the NMC electrodes to get an optimal thickness of coating. The electrochemical cycling performance based on these electrodes is showed in Fig. 3. Fig. 3a shows the discharge performance at a 1C rate between 2.0 V and 4.8 V for the cells based on UC, 2Al_2O_3, 4Al_2O_3, and 6Al_2O_3 coated NMC electrodes at room temperature up to 200 cycles of charge-discharge. The UC NMC delivered an initial discharge capacity of ∼148 mAh/g at a 1C rate, but the capacity kept fading along with the cycling process; after 200 cycles, the capacity declined to ∼40 mAh/g; the decline of capacity could be due to the formation of SPI and migration and dissolution of transition metals.[23] For the 2Al_2O_3 NMC and 4Al_2O_3 NMC electrodes, the initial discharge capacity was ∼168 mAh/g and ∼172 mAh/g, respectively; after 100 cycles of charge-discharge, the discharge capacity remained at ∼142 mAh/g and ∼158 mAh/g, respectively. The increase of discharge capacities

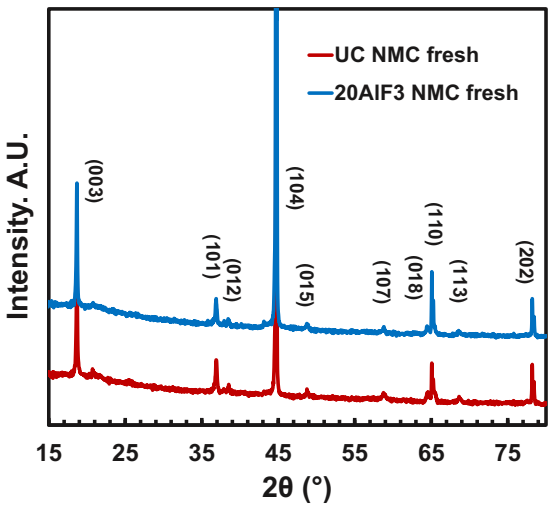

Figure 2. XRD patterns of UC NMC electrode and 20AlF_3 NMC electrode.

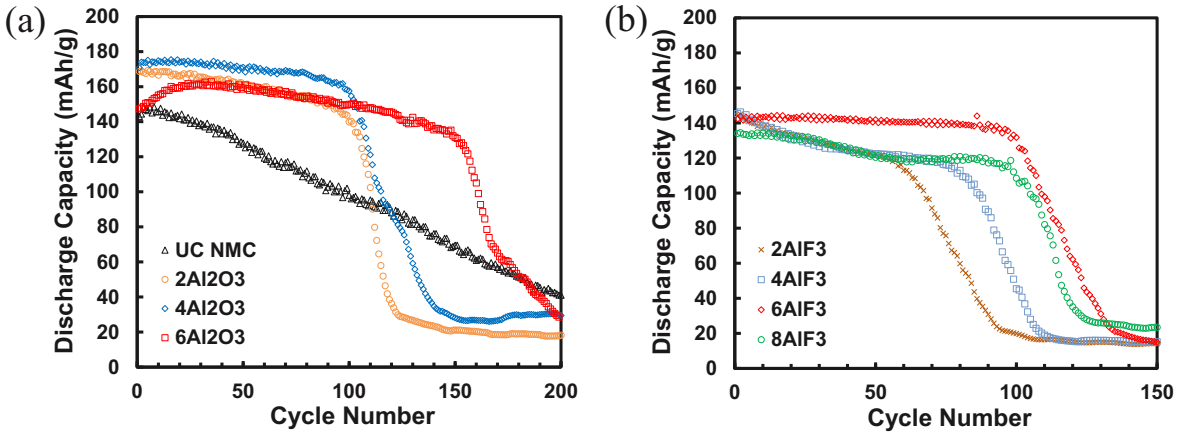

Figure 3. Discharge performance of different cycles (a) Al_2O_3 coated NMC electrodes and (b) AlF_3 coated NMC electrodes.

of the $2Al_2O_3$ NMC and $4Al_2O_3$ NMC electrodes, compared to that of UC NMC, was attributed to the formation of ion conductive Li-Al-O film during charge-discharge process.[24] However, the capacity of $2Al_2O_3$ NMC and $4Al_2O_3$ NMC faded to ~20 mAh/g and ~28 mAh/g after 150 cycles of charge-discharge. These results indicated that the Al_2O_3 coating can enhance the charge-discharge capacity as well as the cycling stability to some level, but it cannot provide a long time protection. The initial discharge capacity of $6Al_2O_3$ NMC was ~147 mAh/g, which was relatively low, compared to those of $2Al_2O_3$ NMC and $4Al_2O_3$ NMC; this was because of the polarization with a thicker film of insulating Al_2O_3. The thicker coating layer can provide a longer time of protection, so the capacity remained at ~137 mAh/g after 150 cycles of charge-discharge; but after that, $6Al_2O_3$ NMC suffered the same problem as $2Al_2O_3$ NMC and $4Al_2O_3$ NMC did. The severe decline of capacity indicated that the coating layer could be depleted by HF from electrolyte.[25]

Fig. 3b shows the discharge performance of the cells based on $2AlF_3$, $4AlF_3$, $6AlF_3$, and $8AlF_3$ coated NMC electrodes at room temperature at a 1C rate between 2.0 V and 4.8V. Similar to those of the Al_2O_3 coated electrodes, all AlF_3 coated NMC showed a short stability enhancement, compared to the performance of the uncoated electrodes. Among them, $6AlF_3$ NMC showed the best performance with an initial capacity of ~143 mAh/g; after 90 cycles of charge-discharge, the capacity remained at ~140 mAh/g with a capacity retention over 95%. The performance of AlF_3 coating was consistent with a previous report that the AlF_3 coating can effectively alleviate the voltage fade in Li-rich NMC materials.[13] However, after less than 100 cycles of charge-discharge, all electrodes suffered sharply capacity decay.

Although surface modification with Al_2O_3 and AlF_3 have achieved some successes to enhance the electrochemical performance in varying levels, Al_2O_3 coating can enhance the capacity by formation of conductive Li-Al-O film, while the coating layer can't resist corrosive of HF from electrolyte. AlF_3 coating can suppress the voltage fade in Li-rich NMC and provide high capacity retention. There is no report to combine both merits of those coatings. In this study, we attempted to coat an ultra-thin film of Al_2O_3 on NMC electrodes to enhance the surface stability without sacrificing electronic conductivity between host material and carbon black, and then a few cycles of AlF_3 ALD films were applied on the uniform Al_2O_3 film surface to enhance the chemical inertia, taking advantages of both Al_2O_3 and AlF_3 to get a more comprehensive enhance.

Fig. 4 shows the performance of discharge cycling at a 1C rate between 2.0 V and 4.8 V for the cells based on UC, $1AlF_3$-$5Al_2O_3$, $2AlF_3$-$4Al_2O_3$, $4AlF_3$-$2Al_2O_3$, and $5AlF_3$-$1Al_2O_3$ coated NMC electrodes at room temperature up to 200 cycles of charge-discharge. The $1AlF_3$-$5Al_2O_3$ sample showed the best performance. The initial discharge capacity of $1AlF_3$-$5Al_2O_3$ and $2AlF_3$-$4Al_2O_3$ was ~147 mAh/g and ~143 mAh/g, respectively; after 200 cycles of charge-discharge, the discharge capacity still remained at ~95 mAh/g and ~120 mAh/g, respectively. The capacity retention of the $1AlF_3$-$5Al_2O_3$ electrode was about 84%, compare to 25% of the uncoated NMC electrode after 200 cycles of charge-discharge. With the increase in the amount of AlF_3 coated on Al_2O_3 layer, the performance of $4AlF_3$-$2Al_2O_3$ and $5AlF_3$-$1Al_2O_3$ samples was more like that of pure AlF_3 coated NMC.

For layered Li-rich NMC, during charge-discharge process, the layered NMC will gradually transform to spinel structure with the increase of cycle number. In order to investigate and determine the capacity degradation of the electrodes, the discharge capacities of the uncoated and coated electrodes were separated into two parts (see Fig. 5), i.e., ">3.5 V" and "<3.5 V". We consider that the capacity above 3.5 V is mainly from the layered structure and the capacity below 3.5 V is mainly from the spinel structure.[26] Fig. 5a shows the capacities provided by a layered structure. The capacities of UC NMC and $6Al_2O_3$ NMC increased slightly during the initial few cycles of charge-discharge, and then kept fading along with the charge-discharge process. The capacities of $6AlF_3$, $1AlF_3$-$5Al_2O_3$, and $2AlF_3$-$4Al_2O_3$ coated NMC electrodes kept decreasing, but slower compared to those of UC NMC and $6Al_2O_3$ NMC. Fig. 5b shows the discharge capacities provided by spinel structure below 3.5V. For UC NMC, the discharge capacity showed a similar tendency with layered structure, slightly increased during the first few cycles and then kept decreasing. For $6Al_2O_3$ NMC, the capacity increased from ~83 mAh/g to ~120 mAh/g for the first 150 cycles and then severely decreased. The increase of capacity should be related to the structure transition from the layered to a spinel-like phase in Li-rich NMC during its

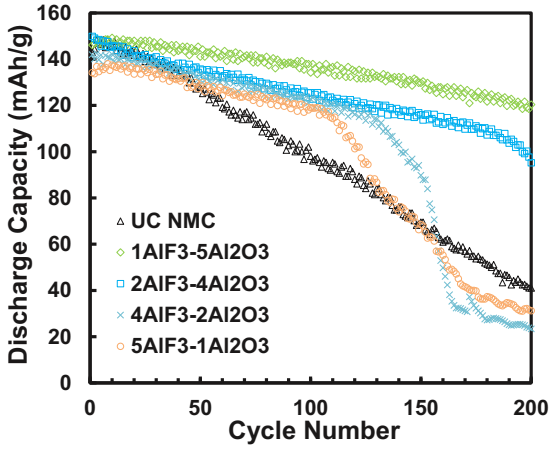

Figure 4. Discharge performance of NMC electrodes with a combination of AlF_3 and Al_2O_3 ALD films.

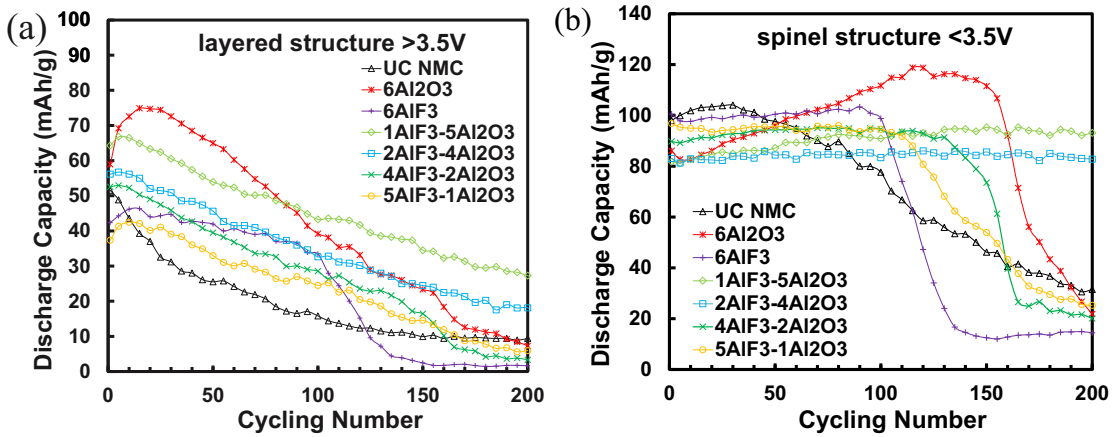

Figure 5. Separated discharge capacities for UC, $6Al_2O_3$, $6AlF_3$, $1AlF_3$-$5Al_2O_3$, $2AlF_3$-$4Al_2O_3$, $4AlF_3$-$2Al_2O_3$, and $5AlF_3$-$1Al_2O_3$ NMC electrodes at a 1 C rate in a voltage range of (a) 3.5V−4.8 V (layered) and (b) 2.0 V−3.5 V (spinel) at room temperature.

repeated charge-discharge cycling.[27] Accompanied by the migration of transition-metal cation into Li vacant sites, the working voltage inevitably decayed. However, for the $6AlF_3$ NMC electrode, the capacity of spinel-like structure and layered structure kept unchanged for the first 100 cycles. The results of these two figures indicate that the AlF_3 coating not only inhibited the side reactions between active material and electrolyte, but also mitigated the transition metal ions moving to lithium vacant sites, which could suppress the structure transition from layered structure to spinel-like structure. For the $2AlF_3$-$4Al_2O_3$ NMC electrode, the capacity of spinel-like structure kept unchanged for 200 cycles (∼82 mAh/g), and the capacity of $1AlF_3$-$5Al_2O_3$ NMC electrode showed a slightly increase for the first 200 cycles, from ∼80 mAh/g to ∼91 mAh/g.

For Li-rich NMC, voltage fade is another aging problem along with the structural transformation during charge-discharge process.[28] We calculated average discharge voltage of UC NMC and all ALD coated NMC by dividing discharge energy by discharge capacity. Fig. 6 shows the discharge voltage of UC NMC and ALD coated NMC electrodes during the charge-discharge process. For all electrodes, the average discharge voltage of the first two cycles are nearly the same, up to 3.5 V, however, after formation, the UC NMC electrode suffered severe voltage fade during subsequent charge-discharge process when charged at a 1C rate, the voltage kept fading from 3.3 V to 2.9 V after 150 cycles of charge-discharge. It was reported that the activated Mn^{3+}/Mn^{4+} and Co^{2+}/Co^{3+} redox couples resulted from oxygen releasing played a critical role in voltage fade.[29] However, for the $1AlF_3$-$5Al_2O_3$ NMC electrode, the voltage fading is much slower than that of UC NMC; after 150 cycles of charge-discharge at a 1C rate, the discharge voltage changed from 3.4 V to 3.2 V, which indicated that the $1AlF_3$-$5Al_2O_3$ coating could suppress oxygen release to provide a higher power density than UC NMC did. Both enhancement of capacity retention and discharge voltage indicated that slightly fluorination of Al_2O_3 coating inherited the merits of both Al_2O_3 coating and AlF_3 coating.

In order to understand how coating enhanced the electrochemical performance of NMC, we studied the initial charge-discharge performance of $1AlF_3$-$5Al_2O_3$ NMC and UC NMC and the change of interfacial layer between electrode and electrolyte after cycling. The initial charge-discharge curves of the UC NMC and $1AlF_3$-$5Al_2O_3$ NMC are shown in Fig. 7. The electrochemical performance was measured at a 0.05 C rate with a cutoff potential of 2.0 V–4.8 V. For both samples,

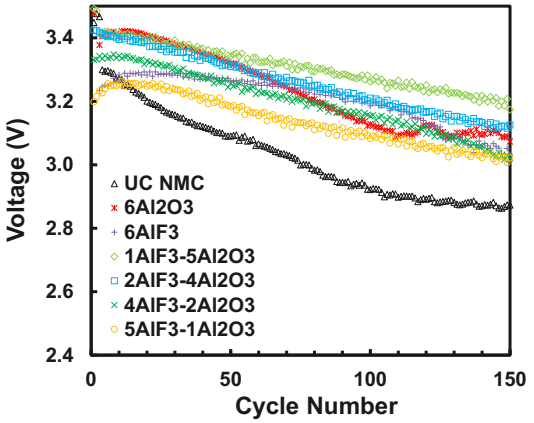

Figure 6. Discharge voltage change of UC, $6Al_2O_3$, $6AlF_3$, $1AlF_3$-$5Al_2O_3$, $2AlF_3$-$4Al_2O_3$, $4AlF_3$-$2Al_2O_3$, and $5AlF_3$-$1Al_2O_3$ ALD coated NMC electrodes.

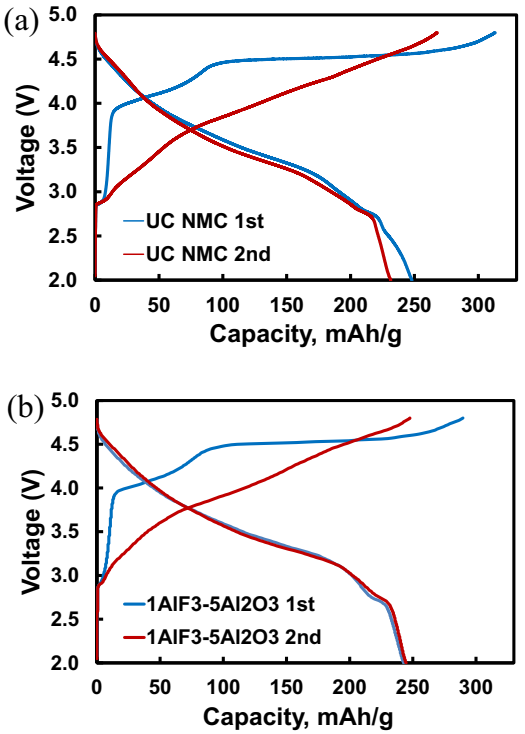

Figure 7. First two cycles of charge-discharge curves of (a) UC NMC electrode and (b) $1AlF_3$-$5Al_2O_3$ NMC electrode.

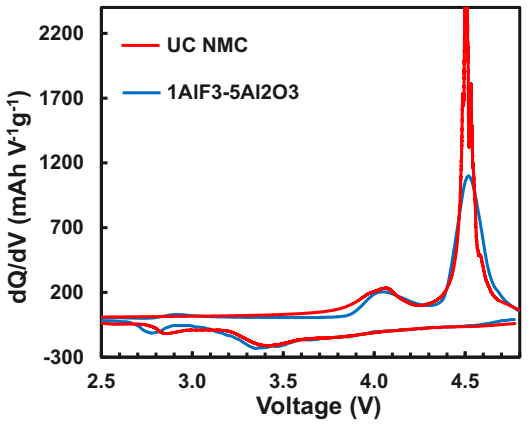

Figure 8. dQ/dV plots for the first charge-discharge cycle of UC NMC electrode and $1AlF_3$-$5Al_2O_3$ NMC electrode.

there was a long potential platform around 4.5 V (vs. Li/Li^+) during the first charge process, and the platform disappeared in the subsequent charge profiles. The reaction mechanism of the initial charge process was reported as the result of lithium ion extracted as Li_2O irreversibly.[30] The initial charge capacity of the $1AlF_3$-$5Al_2O_3$ NMC electrode was slightly lower than that of UC NMC, while the discharge capacity of the second cycle kept nearly unchanged for the coated sample. The coulombic efficiencies of the initial charge-discharge capacities of the UC and $1AlF_3$-$5Al_2O_3$ electrodes were 79.2% and 83.8%, respectively, while the coulombic efficiency of the second cycle of oxides coated NMC was 98.8%, much higher than that of the UC NMC, which was only 86.4%. As the release of Li_2O is irreversible, which leads to lithium vacant sites, resulting in the migration of transition metal ions (e.g., Ni^{4+}) and voltage fading during charge-discharge process. However, the lower charge capacity of the first cycle of the $1AlF_3$-$5Al_2O_3$ NMC electrode indicated that the coating layer could mitigate the release of Li_2O.

The dQ/dV curves of the first charge-discharge cycle of the UC NMC and the $1AlF_3$-$5Al_2O_3$ NMC electrodes are shown in Fig. 8. For both samples, the charge peak at around 4.1 V corresponds to the oxidation of Ni^{2+} to Ni^{4+}. Another sharp peak at 4.5 V is attributed to the removal of oxygen from the crystal structure, which are distinctive resultants of the activation of the Li_2MnO_3 phase. The much stronger peak of the UC NMC electrode, compared to that of the $1AlF_3$-$5Al_2O_3$ NMC electrode at 4.5V, indicates more oxygen release during the first charging process.

To further understand the effects of ALD surface modification on the electrochemical performance of the electrodes, the surface compositions of the fresh UC NMC and $1AlF_3$-$5Al_2O_3$ NMC electrodes, and the electrodes after 100 cycles of charge-discharge were analyzed using XPS. In the C_{1s} XPS spectra (Figs. 9a–9d), several peaks corresponding to the CF_2 (290.5 eV) and CH_2 (285.9 eV) bonds in PVDF and the C-C bonds (284.5 eV) in super P conductive agent could be observed in both fresh UC NMC (Fig. 9a) and fresh $1AlF_3$-$5Al_2O_3$ NMC (Fig. 9c); these two spectra shared similar peaks at the same positions. After charge-discharge for 100 cycles, a sharp peak of C-O single bond at the binding energy of 285.1 eV was observed on UC NMC, which can be attributed to carbonaceous species, mainly from the deposition of electrolyte.[31] Furthermore, the peak value of the super P conductive agent dropped significantly for UC NMC, indicating that a very thick of degradation species covered on the surface of electrode; however, the peaks of PVDF did not show a sharp drop, indicating that the degradation of the electrolyte preferably involved the electrode portion where the electrochemical reaction took place.[32] Since the carbonaceous species are unfavorable components of SPI due to their insulation and instability, we can conclude that one reason of the capacity decay of UC NMC was related to the increase of surface impedance due to the deposition of non-conductive SPI.[33] On the other

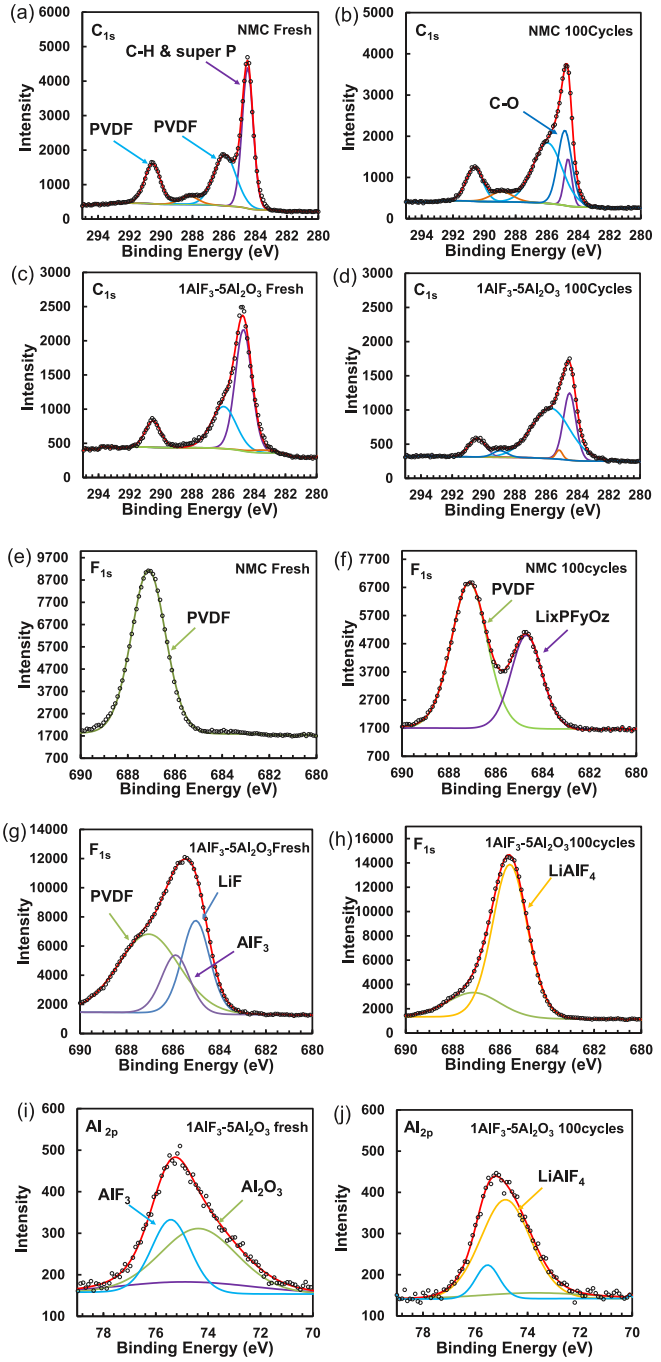

Figure 9. XPS results of C 1s of (a, c) fresh and (b, d) cycled electrodes: (a) fresh UC NMC electrode, (b) cycled UC NMC electrode, (c) fresh $1AlF_3$-$5Al_2O_3$ NMC electrode, (d) cycled $1AlF_3$-$5Al_2O_3$ NMC electrode; XPS results of F 1s of (e, g) fresh and (f, h) cycled electrodes: (e) fresh UC NMC electrode, (f) cycled UN NMC electrode, (g) fresh $1AlF_3$-$5Al_2O_3$ NMC electrode, (h) cycled $1AlF_3$-$5Al_2O_3$ NMC electrode; and XPS results of Al 2p of (i) fresh $1AlF_3$-$5Al_2O_3$ NMC electrode, (j) cycled $1AlF_3$-$5Al_2O_3$ NMC electrode.

hand, there were no distinct additional peaks in the C_{1s} spectra after 100 cycles of charge-discharge, which confirmed the chemical inert of the coating layer and the effective inhibition of the side reactions by the coating.

Figs. 9e–9h illustrate the F_{1s} XPS spectra. Only one type of fluorine (PVDF at 687.1 eV) was observed on UC NMC. However, three types of fluorine were found on the $1AlF_3$-$5Al_2O_3$ NMC electrode. In addition to PVDF and AlF_3, another peak at 685.0 eV belonged

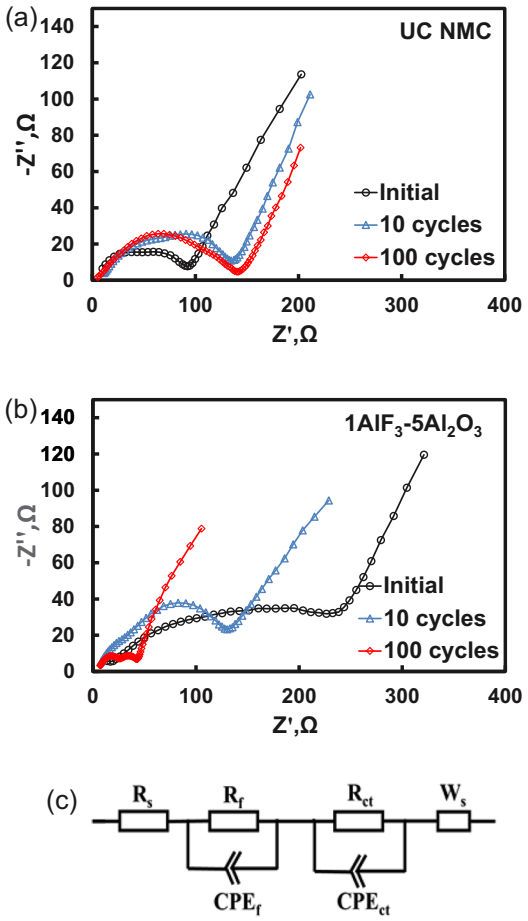

Figure 10. EIS profiles of (a) UC NMC and (b) $1AlF_3$-$5Al_2O_3$ NMC, obtained at a cell potential of 2.9 V (vs Li/Li^+), and (c) the simulated equivalent circuit.

to LiF, indicating that the dosed HF precursor could react with the host materials during the ALD process. Furthermore, after cycling, an additional peak at 684.6 eV was observed on the F_{1s} XPS spectrum of UC NMC. This peak is generally assigned to $Li_xPF_y/Li_xPF_yO_z$, which can be attributed to the degradation of $LiPF_6$ during the cycling process.[32,34,35] The F_{1s} peak of the $1AlF_3$-$5Al_2O_3$ NMC electrode shifted after cycling, and the peak can be deconvoluted into two components. The new peak belonged neither to AlF_3 nor to LiF, but belonged to $LiAlF_4$,[36] and no peak of $Li_xPF_y/Li_xPF_yO_z$ emerged. It indicated that during the cycling process, due to the existence of AlF_3 and LiF, and the lithiation of Al_2O_3, instead of being depleted by the electrolyte, a much more stable $LiAlF_4$ film was formed, which could effectively prevent the electrolyte from decomposing upon cycling. It also explains the reason why $1AlF_3$-$5Al_2O_3$ coating can provide a much longer protection than pure Al_2O_3 coating or AlF_3 coating did.

Figs. 9i–9j illustrate the Al_{2p} XPS spectra of the $1AlF_3$-$5Al_2O_3$ NMC electrode. Two peaks corresponding to AlF_3 and Al_2O_3 can be deconvoluted from the Al_{2p} XPS spectra of fresh coated sample.[17] After 100 cycles of charge-discharge, the peak areas of both AlF_3 and Al_2O_3 decreased sharply, and a strong peak of $LiAlF_4$ verified that upon cycling; AlF_3 and Al_2O_3 were driven to transform into $LiAlF_4$. The XPS spectra results of Al_{2p} are consistent with the results of F_{1s}.

To further insight the origins of electrochemical performance improvement, EIS of UC NMC and $1AlF_3$-$5Al_2O_3$ NMC were tested, respectively, before charge-discharge and after charge-discharge for 10 and 100 cycles at 2.9 V (vs. Li/Li^+), as shown in Fig. 10. The impedance spectra (Nyquist plots) consist of two semicircles and an inclined line: the two semicircles are in the high frequency and intermediate frequency ranges, and the inclined line at a constant angle to the abscissa. The first semicircle at the high frequency is attributed to the lithium ions migration through the surface film, and the second semicircle of the intermediate frequency comes from the interfacial charge transfer reaction. The inclined line is the result of lithium ion diffusion into the active host materials.[37,38]

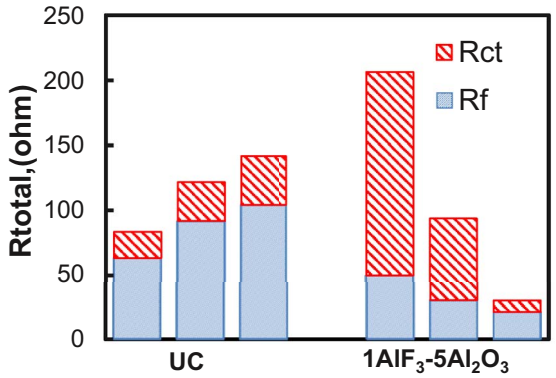

Figure 11. Summary of fitted parameters, R_f and R_{ct}, at 0^{th} cycle (left) 10^{th} cycle (middle) and 100^{th} cycle (right).

The impedance spectra were fitted using a simplified equivalent circuit. The resistance (R_s) represents the uncompensated ohmic resistance. The first pair of resistance (R_f) and constant phase element (CPE) represent lithium migration occurring through the surface film region. The second pair of resistance (R_{ct}) and CPE are the indicative of charge-transfer resistance and double layer capacitance. The Warburg impedance (W_s), represents the solid-state diffusion reaction. All the electrical parameters in the equivalent circuit were determined from the CNLS (complex nonlinear least-squares) fitting method, as shown in Fig. 11.

For UC NMC, the initial R_f and R_{ct} were about 63 Ω and 21 Ω; after 10 cycles of charge-discharge, the R_f and R_{ct} increased to 91 Ω and 28 Ω, respectively, indicating that SPI was formed on the surface of electrodes due to side reactions between the surface and electrolyte. For UC NMC, the smallest values of the charge-transfer resistance and semi-infinite diffusion impedance appeared after formation, while the maximum discharge capacity can be obtained. With continuous cycling, the structural integrity of the Li-rich layered oxides was compromised. As a result, the diffusion impedance and the surface charge-transfer resistance increase gradually,[39] as shown in Fig. 11. For $1AlF_3$-$5Al_2O_3$ NMC, the initial resistance R_f (50 Ω) and R_{ct} (156 Ω) were much higher than those of UC NMC, due to the generation of lower conductive LiF during the ALD process, as verified by XPS analysis; however, both of those two resistances decreased along with the charge-discharge cycling, suggesting that electrolyte decomposition at high voltage operation and manganese ion dissolution have been curtailed, which was due to the formation of more stable and conductive $LiAlF_4$ film; this is consistent with the results of XPS. Furthermore, the suppression of phase transition from layer structure to spinel structure also contributed to the decrease of impedance.

Conclusions

To summarize, a composite film consisting of AlF_3 and Al_2O_3 was coated on Li-rich NMC electrodes by ALD. This coating with optimal composition and thickness inherited both merits of AlF_3 coating and Al_2O_3 coating, and demonstrated effective protection for the cathode material against the attack from the electrolyte. By suppressing side reactions between the electrolyte and electrode, inhibiting the transformation of layered Li_2MnO_3 into a spinel-like phase, and reducing the oxygen release during initial charge, the electrochemical performance of the $1AlF_3$-$5Al_2O_3$ coated NMC electrodes showed significant improvement, compared to that of UC NMC electrodes. The transformation of coating layer during charge-discharge cycling, helped

create a more robust and Li ion conductive SPI layer, which made both the cycling stability and voltage stability of the $1AlF_3$-$5Al_2O_3$ coated NMC electrode better than those of pure Al_2O_3 coated NMC electrodes or pure AlF_3 coated NMC electrodes. This study indicates that a protective layer between electrode and electrolyte with better properties can be achieved by a reasonable combination of different coating layers. This strategy can be used to other kinds of films to help improve the performance of lithium ion batteries with higher output voltage, higher energy density, and longer life span.

Acknowledgments

This work was supported in part by the National Science Foundation grant NSF DMR 1464111.

ORCID

Han Yu https://orcid.org/0000-0001-6965-4000
Xinhua Liang https://orcid.org/0000-0001-7979-0532

References

1. Y.-K. Sun, S.-T. Myung, B.-C. Park, J. Prakash, I. Belharouak, and K. Amine, *Nature Materials*, **8**, 320 (2009).
2. P. Yan, J. Zheng, J. Xiao, C.-M. Wang, and J.-G. Zhang, *Frontiers in Energy Research*, **3**, 26 (2015).
3. H. Yu and H. Zhou, *The Journal of Physical Chemistry Letters*, **4**, 1268 (2013).
4. J. B. Goodenough and K.-S. Park, *Journal of the American Chemical Society*, **135**, 1167 (2013).
5. M. M. Thackeray, S.-H. Kang, C. S. Johnson, J. T. Vaughey, R. Benedek, and S. Hackney, *Journal of Materials Chemistry*, **17**, 3112 (2007).
6. J.-H. Lim, H. Bang, K.-S. Lee, K. Amine, and Y.-K. Sun, *Journal of Power Sources*, **189**, 571 (2009).
7. C. Johnson, J. Kim, C. Lefief, N. Li, J. Vaughey, and M. Thackeray, *Electrochemistry Communications*, **6**, 1085 (2004).
8. S.-H. Kang and M. M. Thackeray, *Electrochemistry Communications*, **11**, 748 (2009).
9. K. W. Nam, S. M. Bak, E. Hu, X. Yu, Y. Zhou, X. Wang, L. Wu, Y. Zhu, K. Y. Chung, and X. Q. Yang, *Advanced Functional Materials*, **23**, 1047 (2013).
10. D. Aurbach, Y. Talyosef, B. Markovsky, E. Markevich, E. Zinigrad, L. Asraf, J. S. Gnanaraj, and H.-J. Kim, *Electrochimica Acta*, **50**, 247 (2004).
11. M. Jiang, B. Key, Y. S. Meng, and C. P. Grey, *Chemistry of Materials*, **21**, 2733 (2009).
12. B. Xu, C. R. Fell, M. Chi, and Y. S. Meng, *Energy & Environmental Science*, **4**, 2223 (2011).
13. J. Zheng, M. Gu, J. Xiao, B. J. Polzin, P. Yan, X. Chen, C. Wang, and J.-G. Zhang, *Chemistry of Materials*, **26**, 6320 (2014).
14. Z. Wang, E. Liu, C. He, C. Shi, J. Li, and N. Zhao, *Journal of Power Sources*, **236**, 25 (2013).
15. Y. Wu, A. V. Murugan, and A. Manthiram, *Journal of The Electrochemical Society*, **155**, A635 (2008).
16. H.-M. Cho, M. V. Chen, A. C. MacRae, and Y. S. Meng, *ACS Applied Materials & Interfaces*, **7**, 16231 (2015).
17. J. W. Kim, D. H. Kim, D. Y. Oh, H. Lee, J. H. Kim, J. H. Lee, and Y. S. Jung, *Journal of Power Sources*, **274**, 1254 (2015).
18. Q. Wang, J. Liu, A. V. Murugan, and A. Manthiram, *Journal of Materials Chemistry*, **19**, 4965 (2009).
19. Y. K. Sun, M. J. Lee, C. S. Yoon, J. Hassoun, K. Amine, and B. Scrosati, *Advanced Materials*, **24**, 1192 (2012).
20. F. Ding, W. Xu, D. Choi, W. Wang, X. Li, M. H. Engelhard, X. Chen, Z. Yang, and J.-G. Zhang, *Journal of Materials Chemistry*, **22**, 12745 (2012).
21. J. Ding, Z. Lu, M. Wu, C. Liu, H. Ji, and G. Yang, *Applied Surface Science*, **406**, 21 (2017).
22. Y. Lee, H. Sun, M. J. Young, and S. M. George, *Chemistry of Materials*, **28**, 2022 (2016).
23. P. Rozier and J. M. Tarascon, *Journal of The Electrochemical Society*, **162**, A2490 (2015).
24. Y. Liu, N. S. Hudak, D. L. Huber, S. J. Limmer, J. P. Sullivan, and J. Y. Huang, *Nano Letters*, **11**, 4188 (2011).
25. Z. Chen, Y. Qin, K. Amine, and Y.-K. Sun, *Journal of Materials Chemistry*, **20**, 7606 (2010).
26. B. Song, Z. Liu, M. O. Lai, and L. Lu, *Physical Chemistry Chemical Physics*, **14**, 12875 (2012).
27. Y. Gao, R. L. Patel, K.-Y. Shen, X. Wang, R. L. Axelbaum, and X. Liang, *ACS Omega*, **3**, 906 (2018).
28. D. Mohanty, J. Li, D. P. Abraham, A. Huq, E. A. Payzant, D. L. Wood III, and C. Daniel, *Chemistry of Materials*, **26**, 6272 (2014).
29. E. Hu, X. Yu, R. Lin, X. Bi, J. Lu, S. Bak, K.-W. Nam, H. L. Xin, C. Jaye, and D. A. Fischer, *Nature Energy*, **3**, 690 (2018).
30. J. Yan, X. Liu, and B. Li, *Rsc Advances*, **4**, 63268 (2014).
31. L. Yang and B. L. Lucht, *Electrochemical and Solid-State Letters*, **12**, A229 (2009).
32. H. Bouayad, Z. Wang, N. Dupre, R. Dedryvère, D. Foix, S. Franger, J.-F. Martin, L. Boutafa, S. Patoux, and D. Gonbeau, *The Journal of Physical Chemistry C*, **118**, 4634 (2014).
33. B. Xiao, B. Wang, J. Liu, K. Kaliyappan, Q. Sun, Y. Liu, G. Dadheech, M. P. Balogh, L. Yang, and T.-K. Sham, *Nano Energy*, **34**, 120 (2017).
34. Y.-C. Lu, A. N. Mansour, N. Yabuuchi, and Y. Shao-Horn, *Chemistry of Materials*, **21**, 4408 (2009).
35. T. Eriksson, A. Andersson, C. Gejke, T. Gustafsson, and J. O. Thomas, *Langmuir*, **18**, 3609 (2002).
36. J. Xie, A. D. Sendek, E. D. Cubuk, X. Zhang, Z. Lu, Y. Gong, T. Wu, F. Shi, W. Liu, and E. J. Reed, *ACS Nano*, **11**, 7019 (2017).
37. F. Kuang, D. Zhang, Y. Li, Y. Wan, and B. Hou, *Journal of Solid State Electrochemistry*, **13**, 385 (2009).
38. M. Gaberscek, J. Moskon, B. Erjavec, R. Dominko, and J. Jamnik, *Electrochemical and Solid-State Letters*, **11**, A170 (2008).
39. G. Li, X. Feng, Y. Ding, S. Ye, and X. Gao, *Electrochimica Acta*, **78**, 308 (2012).